

Geometric Phase in Quantum Billiards with a Pointlike Scatterer

Taksu Cheon

Department of Physics, Hosei University, Fujimi, Chiyoda-ku, Tokyo 102, Japan

Takaomi Shigehara

Computer Centre, University of Tokyo, Yayoi, Bunkyo-ku, Tokyo 113, Japan

(July 28, 1995)

Abstract

We examine the quantum energy levels of rectangular billiards with a pointlike scatterer in one and two dimensions. By varying the location and the strength of the scatterer, we systematically find diabolical degeneracies among various levels. The associated Berry phase is illustrated, and the existence of localized wave functions is pointed out. In one dimension, even the ground state is shown to display the sign reversal with a mechanism to circumvent the Sturm-Liouville theorem.

03.65.Bz, 05.45.+b, 42.50.Dv

arXiv:hep-th/9512164v1 20 Dec 1995

A sense of mystery has accompanied the geometric phase from the day of its discovery [1,2]. It has deepened when the connection between the geometric phase and the gauge field has been recognized [3]. Although there are several model systems in relatively simple settings, few qualify as transparent examples that give us the intuition into the origin and the workings of the geometric phase.

In this Letter, we examine the candidates for just such examples. We study the bound state problem in a rectangular billiard with a pointlike scatterer inside. The zero-size scatterer is an idealized limit of a small obstacle. In this limit, the solution of the problem is expected to be simplified substantially. That simplification is indeed realized when the divergence caused by the singularity of the interaction is handled properly with the self-adjoint extension theory of functional analysis [4-7]. We look at the energy level structure of this system along with its one-dimensional analogue. We point out the existence of a set of diabolical points and of associated geometric phase. An examination of wave functions around the diabolical points also reveals the emergence of unexpectedly localized wave functions.

We first consider a one-dimensional delta potential problem with the Dirichlet boundary condition (vanishing wave function) at $x = 0$ and 1. We place a pointlike scatterer of strength $1/s$ at $x = x_0$:

$$V = \frac{1}{s} \delta(x - x_0). \quad (1)$$

The diagonal element of the free Green's function at $x = x_0$ is given by

$$G(\omega) = \sum_{n=1}^{\infty} \frac{\varphi_n^2(x_0)}{\omega - \varepsilon_n} \quad (2)$$

where $\varepsilon_n = \pi/4 \cdot n^2$ and $\varphi_n(x) = \sqrt{2} \sin(n\pi x)$ ($n = 1, 2, \dots$) are the eigenvalues and eigenfunctions of the unperturbed system. (We chose the mass to be 2π .) The eigenvalues of the problem with the delta function are given as the solutions of the equation

$$G(\omega) - s = 0. \quad (3)$$

The eigenfunction (apart from the normalization) corresponding to an eigenvalue ω_α is given by

$$\psi_\alpha(x) = \sum_{n=1}^{\infty} \frac{\varphi_n(x_0)}{\omega_\alpha - \varepsilon_n} \varphi_n(x). \quad (4)$$

In Fig.1, we plot the first six eigenvalues at several x_0 as a function of s . Fig. 1 (a) shows the existence of level crossings at infinite strength $s = 0$ with $x_0 = 0.5$. Fig. 1 (b) displays avoided crossings around $s = 0$ for $x_0 = 0.47$, indicating that the crossings at $x_0 = 0.5$ are diabolical. That this is indeed the case is proved by examining Fig. 2 (a), where we display wave functions at various values of (x_0, s) around the point $(0.5, 0)$ starting from the ground state at $(0.5, 0.1)$. By going round the point $(0.5, 0)$, the wave function experiences the Herzberg-Longuet-Higgins sign reversal [8], which is a special case (co-dimension two) of the Berry's geometric phase for real symmetric Hamiltonians. The mechanism of the sign reversal in this simplest of all examples is easy to comprehend: It is a consequence of two conflicting ways of connecting nodeless and one-node wave functions.

At first sight, this result seems to contradict with the Sturm-Liouville theorem of no-crossing and no-node [9], which states that in one dimension there is no level crossing and the ground state always stays nodeless. However, at the diabolical point $(x_0, s) = (0.5, 0)$, the strength of the potential is infinite, where the no-crossing theorem does not have to hold. Also, as seen in Fig. 1, the ground state at $s > 0$ side is smoothly connected to the second state with one node at $s < 0$ side. This happens because when one goes from positive to negative s , a disconnected level appears from the negative infinity to become the ground state for $s < 0$. In this rather tricky manner, the ground state of $s > 0$ side is permitted to acquire the sign reversal through the rotation around the diabolical point.

Looking at Fig. 1 (a), we notice that there are a series of pairwise degeneracies at $(x_0, s) = (0.5, 0)$. This occurs between the states with even n which are unaffected by the delta potential at the center and the states with odd n which lie next to them. Similarly, one realizes from Fig. 1 (c)-(e) that the third state, sixth state, ninth state, *etc.* get crossed by the states next to them at $(x_0, s) = (1/3, 0)$. More generally, if one assumes that N and M are the relative primes satisfying $N > M > 0$, the location $(x_0, s) = (M/N, 0)$ is a diabolical point for the $(N - 1)$ -th and N -th states, $(2N - 1)$ -th and $2N$ -th states, *etc.* (all counted

at $s > 0$ side). Clearly, one exhausts all the level crossings of the system in this manner. We show in Fig. 2 (b), the morphosis of the eighth wave function around the diabolical point $(x_0, s) = (1/9, 0)$. A noteworthy feature is in the middle right figure ($s_0 \simeq 0$ and x_0 slightly larger than $1/9$), where one observes a wave function highly localized between one edge and the location of the delta potential. One can generalize this result: By placing a strong delta potential at an appropriate location, one can obtain a wave function which is localized arbitrary sharply near the edge.

We next treat the case of two dimension. We consider a quantum particle of mass 2π moving inside a rectangle surrounded by the boundaries $x = 0$, $x = R$, $y = 0$ and $y = 1/R$, on which the wave function is assumed to vanish. The eigenstates for this empty billiard problem is given by $\varphi_{nm}(x, y) = 2 \sin(n\pi x/R) \cdot \sin(m\pi yR)$ and their energies $\varepsilon_{nm} = \pi/4 \cdot (n^2/R^2 + m^2R^2)$ ($n, m = 1, 2, \dots$). We place a pointlike scatterer at (x_0, y_0) . Naively, we would have the two-dimensional analogue of eqs. (1) - (3). However, this is not possible since the infinite sum

$$G(\omega) = \sum_{n,m=1}^{\infty} \frac{\varphi_{nm}^2(x_0, y_0)}{\omega - \varepsilon_{nm}} \quad (5)$$

diverges logarithmically because of the constant density of states per unit energy. Instead, we resort to the self-adjoint extension theory of functional analysis. We refer to Ref. [7] for a fuller treatment of the problem, and simply start from the results obtained there. The eigenvalues of the full problem are given by the solutions of

$$\overline{G}(\omega) - \bar{s} = 0 \quad (6)$$

where

$$\overline{G}(\omega) = \sum_{n,m=1}^{\infty} \varphi_{nm}^2(x_0, y_0) \left[\frac{1}{\omega - \varepsilon_{nm}} + \frac{\varepsilon_{nm}}{\varepsilon_{nm}^2 + 1} \right] \quad (7)$$

is the regularized version of $G(\omega)$, and \bar{s} , which we call *formal* inverse strength, is a real number specifying the nature of the pointlike scatterer. The equation (6) can be interpreted as the renormalized eigenvalue equation if \bar{s} is identified as the inverse of the renormalized

coupling strength. In one dimension, we can consider an analogous equations to eqs.(6) and(7). In this case, however, each term in the bracket of eq.(7) converges separately. This allows us to define the inverse strength s in terms of \bar{s} as a finite quantity. This is the reason why we are able to deal with the delta potential in one dimension without any difficulty. The eigenfunction corresponding to a solution ω_α of eq.(6) is given by

$$\psi_\alpha(x, y) = \sum_{n,m=1}^{\infty} \frac{\varphi_{nm}(x_0, y_0)}{\omega_\alpha - \varepsilon_{nm}} \varphi_{nm}(x, y). \quad (8)$$

We look at the energy of the system as a function of the location of the scatterer, (x_0, y_0) with fixed value of \bar{s} . Because of the mirror symmetry of the system, it is sufficient to consider the area $x_0 \in [0, R/2]$ and $y_0 \in [0, 1/(2R)]$. In Fig. 3, we show the energy of the lowest eleven levels as a function of y_0 with $x_0 = 0.5R$ for Fig. 3 (a), and with $x_0 = 0.48R$ for Fig. 3 (b). The value of R is set to $\pi/e \simeq 1.1557273$. The formal inverse strength is chosen to $\bar{s} = 1/10$. Six diabolical crossings can be spotted in Fig. 3 (including the one between the eighth and ninth states which might require further magnification to see the avoided crossing off $x_0 = 0.5R$). All the crossings involve a state with even n , which is unaffected by the presence of the scatterer because of its node line along $x_0 = 0.5R$. As a result, these states appear flat in Fig. 3 (let us call these flat energies of unaffected states ε_φ collectively).

In general, the level crossing in the system with pointlike scatterer can occur only when one of the eigenstates is unaffected by the scatterer. This occurs either along the line $x_0 = (M/N)R$ or along $y_0 = M/(NR)$ where N and M are the relative primes satisfying $N > M > 0$. There, unperturbed wave functions with $(N - 1)$ nodes in x (or y) direction become the solutions of the full problem. The other coordinate y_0 (or x_0) of the crossing point is then determined by eq. (6) with $\omega = \varepsilon_\varphi$. Thus we have a systematic way of locating all diabolical crossings. As we vary R , the diabolical locations move along $x_0 = (M/N)R$ or $y_0 = M/(NR)$. An interesting case is the right square $R = 1$, where the lowest diabolical point (between the second and third states) moves to the center $(x_0, y_0) = (0.5, 0.5)$. We observe *no sign reversal* around this point because this and the other diabolical point at its

mirror location $y'_0 = 1/R - y_0$ merge to form a degenerate diabolical point with the Berry phase 2π .

Going back to the specific case of $R = \pi/e$, we display, in Fig.4, the profile of eigenfunctions around two of the diabolical points; (a) $(x_0, y_0) = (0.5R, 0.3177/R)$ involving the second and third states and (b) $(x_0, y_0) = (0.5R, 0.3875/R)$ for the tenth and eleventh states. In case of (a), the third state keeps the unperturbed quantum numbers $(n, m) = (2, 1)$ and the energy $\varepsilon_\varphi \simeq 3.4$, while in case of (b), the tenth state has $(n, m) = (4, 2)$ and $\varepsilon_\varphi \simeq 13.6$. As in one dimension, we learn from these examples that the sign reversal is a result of two conflicting ways to connect wave functions with different node structures. One can also look at this sign reversal as a rotation of the wave function by 180 degree while the pointlike scatterer makes the full turn of 360 degree. As in one dimension, we observe the appearance of localized wave functions around the diabolical level crossings. Its possible relevance to the “scarring” phenomena [10,11] is an interesting open problem.

Finally, we view our findings from a perspective and discuss their potential utilities. It is important to notice that the rectangular shape of the billiard is a matter of our technical choice than the necessary condition for the occurrence of the diabolical crossings. In fact, by linearizing $\overline{G}(\omega)$ in the neighborhood of ε_φ in eq. (6), we obtain a second-order algebraic equation, with which we can prove the appearance of the Berry phase around diabolical points without any reference to unperturbed eigenfunctions. Therefore, we conclude that a generic system with a pointlike scatterer possesses diabolical crossings and the associated Berry phase. Also, the diabolical crossing discussed here is not a result of the mathematical abstraction inherent in a pointlike scatterer. Indeed, we can show through numerical Fourier-basis diagonalization that the sign reversal is observed in a billiard with a polygonal obstacle of finite size such as the one discussed in Ref. [12]. When the size of the obstacle is small, the diabolical crossing occurs at a location close to the one predicted for a pointlike scatterer. In this case, however, there is no systematic way to locate the diabolical points exactly. It is the very pointlike nature of the obstacle that allows the simple expressions such as eqs. (6) and (7). We can further hope that the simplicity of the formulation of the pointlike

scatterer opens up the possibility of various analytical results concerning the nature of the diabolical points such as their geometrical and statistical properties.

The primary utility of our examples might be a pedagogical one. This is evident when we compare them with the earlier examples of the Berry phase in triangular billiards [13]. The rotation in parameter space in our examples literally is the rotation of a pointlike scatterer in the coordinate space. Also, the occurrence of the diabolical crossing at the lowest possible states including the ground state makes the resulting Berry phase understood in a pictorial, intuitive manner. We can also contemplate a possible use of diabolical crossings in mesoscopic devices. There may be a situation where an obstacle (or impurity) needs to be placed in a certain precise location of the device. This can be achieved by monitoring the degenerate resonance energies while moving the obstacle. Another more fanciful use may be realized when the phase of wave functions becomes utilized. A quantum state with required phase can be obtained by “Berry rotating” an obstacle around its diabolical location.

We acknowledge our gratitude to Prof. M. V. Berry for his suggestion which has led to the conception of this work. We also thank Prof. H. Terazawa for his careful reading of the manuscript and useful comments. T.C. expresses the gratitude to the members of the Theory Division of the Institute for Nuclear Study, University of Tokyo for offering him a friendly and stimulating research environment. T. S. acknowledges the support of the Grant-in-Aid for Encouragement of Young Scientists (No. 07740316) by the Ministry of Education, Science, Sports and Culture of Japan.

REFERENCES

- [1] M. V. Berry, Proc. Roy. Soc. Lond. **A392**, 43 (1984).
- [2] Y. Aharonov and J. Anandan, Phys. Rev. Lett. **58**, 1593 (1987).
- [3] F. Wilczek and A Zee, Phys. Rev. Lett. **52**, 2111 (1984).
- [4] S. Albeverio, F. Gesztesy, R. Høegh-Krohn and H. Holden, *Solvable Models in Quantum Mechanics* (Springer, Berlin, 1988).
- [5] J. Zorbas, J. Math. Phys. **21**, 840 (1980).
- [6] P. Šeba and K. Życzkowski, Phys. Rev. **A44**, 3457 (1991).
- [7] T. Shigehara, Phys. Rev. **E50**, 4357 (1994).
- [8] G. Herzberg and H. C. Longuet-Higgins, Discuss. Faraday Soc. **35**, 77 (1963).
- [9] R. Courant and D. Hilbert, *Methoden der Mathematischen Physik* (Springer, Berlin, 1931).
- [10] E. Heller, Phys. Rev. Lett. **53**, 1515 (1984).
- [11] E. B. Bogomolny, Physica **31D**, 169 (1989).
- [12] T. Cheon and T. D. Cohen, Phys. Rev. Lett. **62**, 2769 (1989).
- [13] M. V. Berry and M. Wilkinson, Proc. Roy. Soc. Lond. **A392**, 15 (1984).

FIGURES

FIG. 1. Six lowest eigenvalues as function of the inverse strength of the delta potential in one dimension: (a) $x_0 = 0.5$, (b) $x_0 = 0.47$, (c) $x_0 = 0.35$, (d) $x_0 = 0.333$ and (e) $x_0 = 0.31$.

FIG. 2. The change of the wave function eq. (4) displaying the Berry phase with various values of (x_0, s) around the diabolic points (a) $(x_0, s) = (1/2, 0)$ and (b) $(x_0, s) = (1/9, 0)$

FIG. 3. Eleven lowest eigenvalues as function of the perpendicular position of the delta potential in two-dimensional billiard while keeping its horizontal position (a) at the center $x_0 = 0.5R$, and (b) slightly off the center $x_0 = 0.48R$. Other parameters are set to $R = 1.1557273$ and $\bar{s} = 0.1$.

FIG. 4. The change of the wave function displaying the Berry phase around the diabolical points (a) $(x_0, y_0) = (0.5R, 0.3177/R)$ and (b) $(x_0, y_0) = (0.5R, 0.3875/R)$ with $R = 1.1557273$ and $\bar{s} = 0.1$. The solid and broken lines indicate positive and negative equilateral lines respectively.

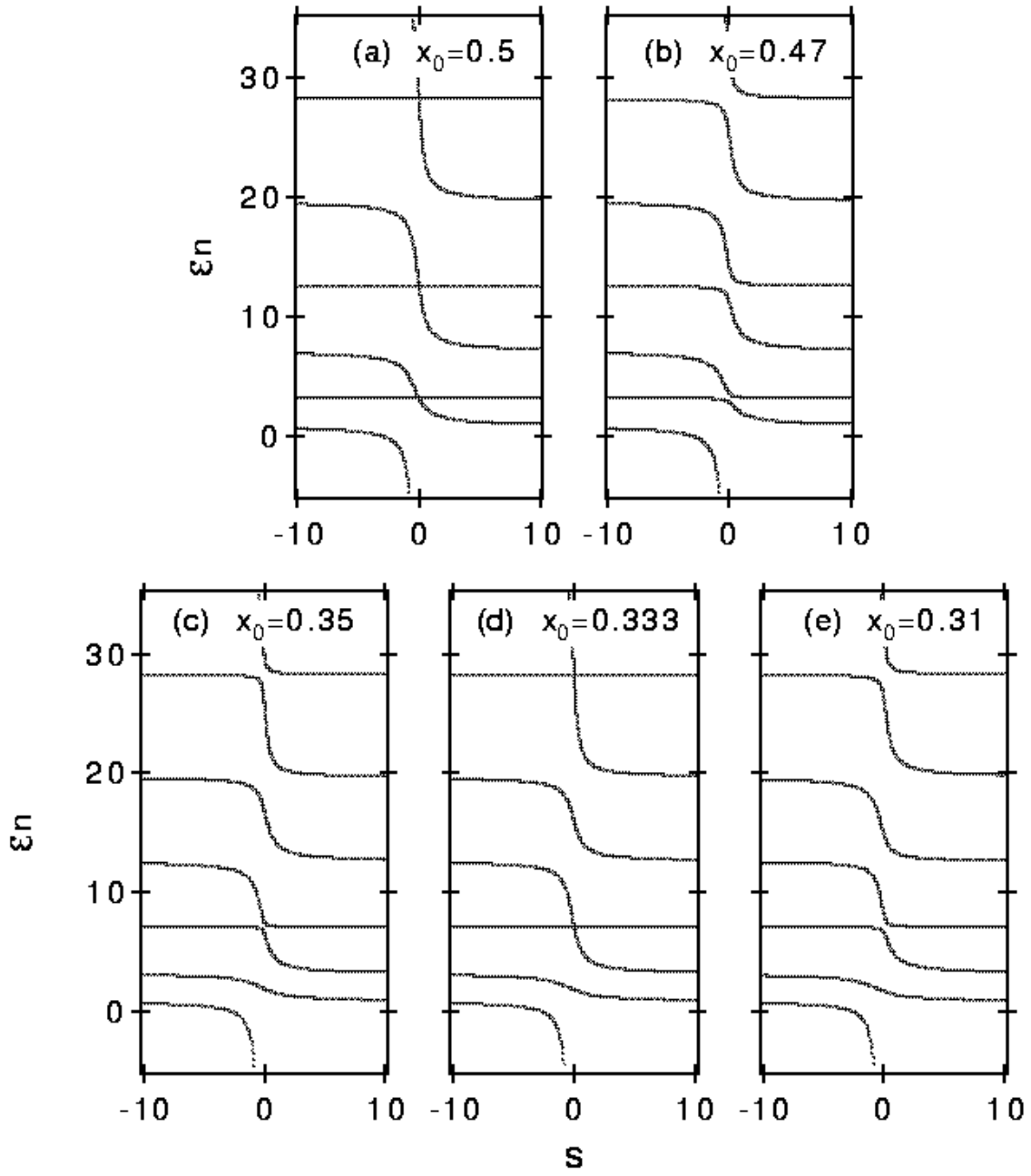


Fig. 1

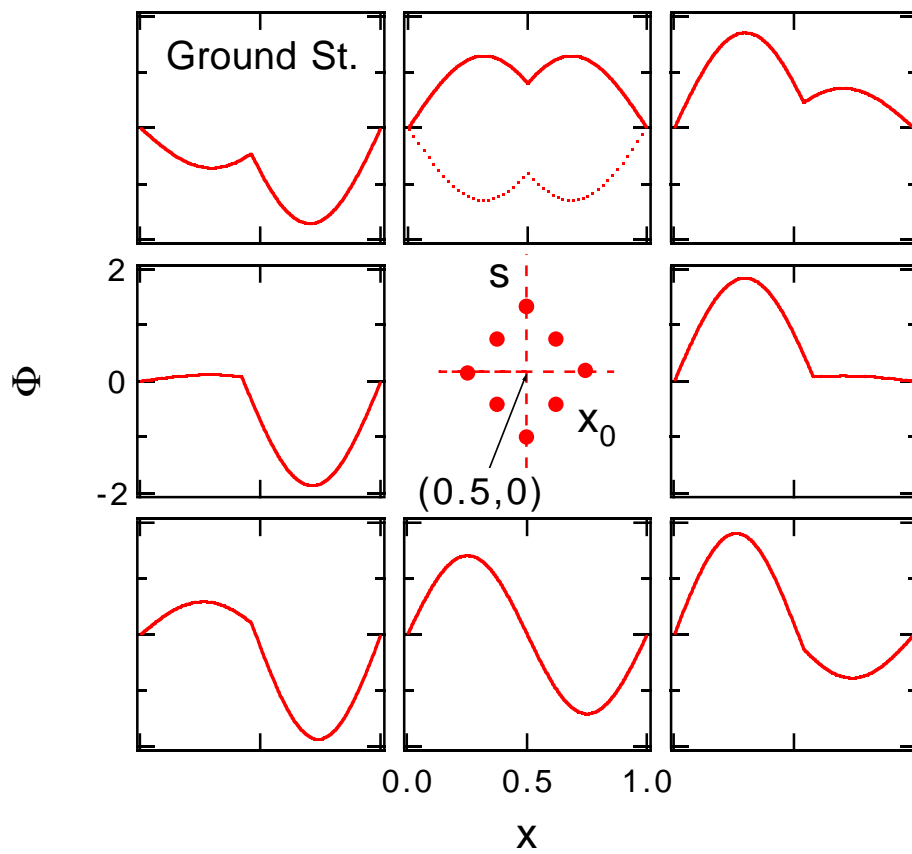


Fig. 2a

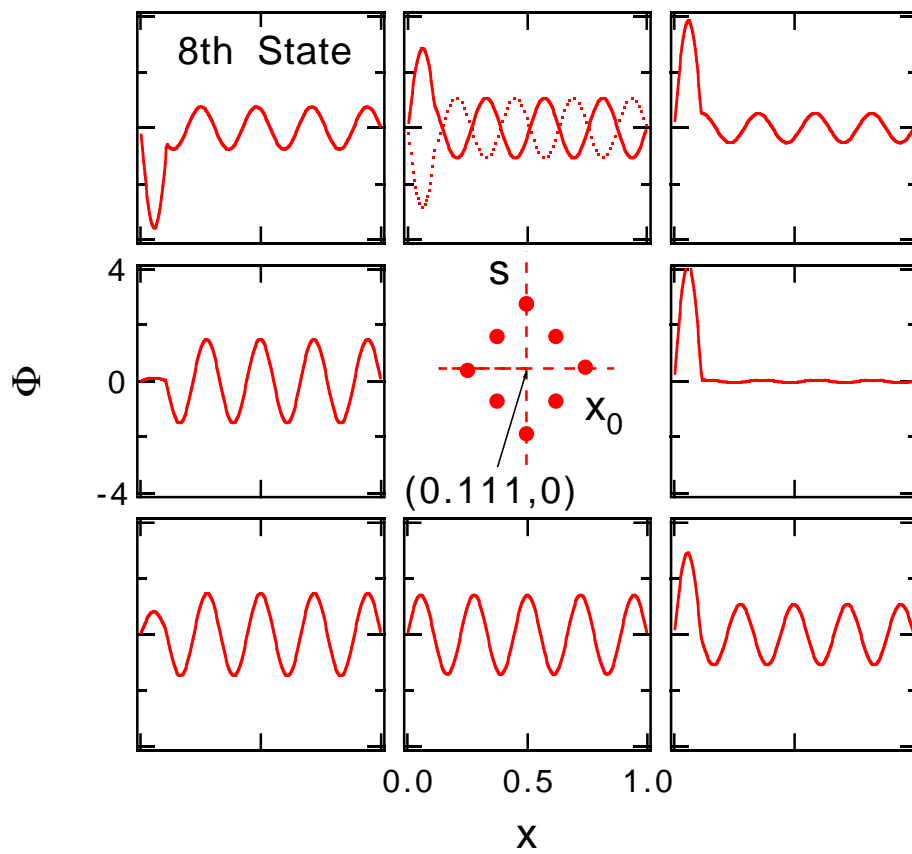


Fig. 2b

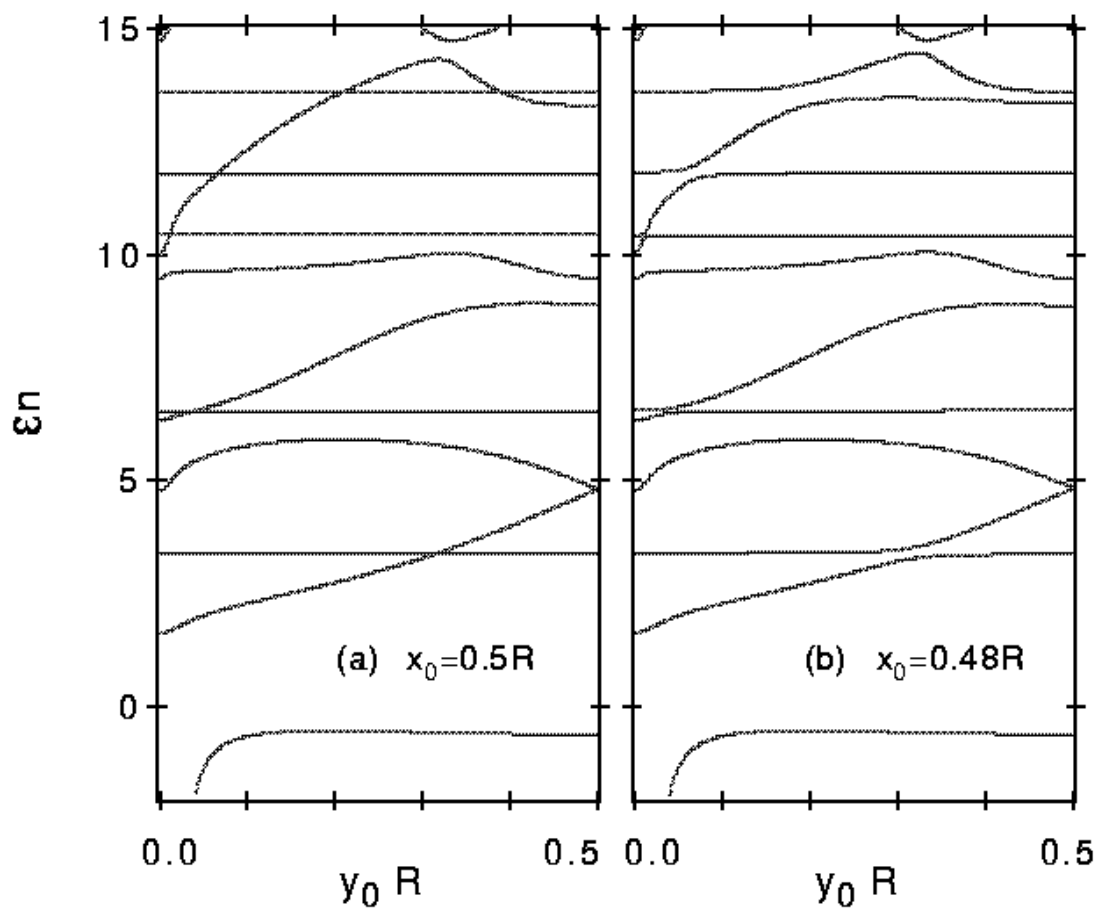


Fig. 3

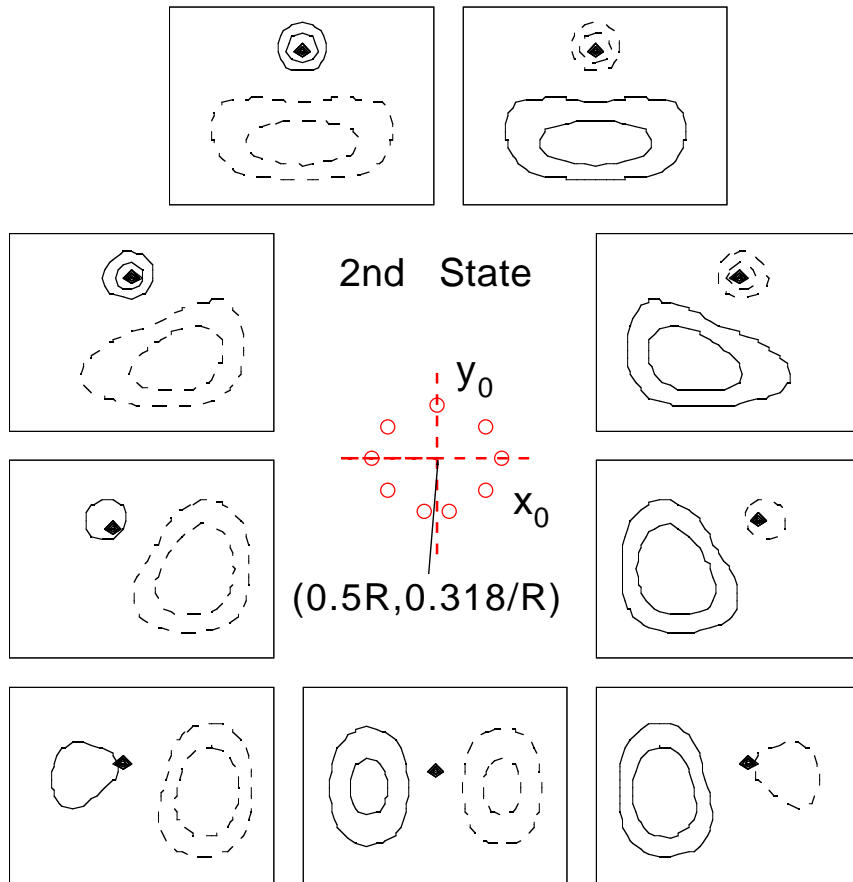


Fig. 4a

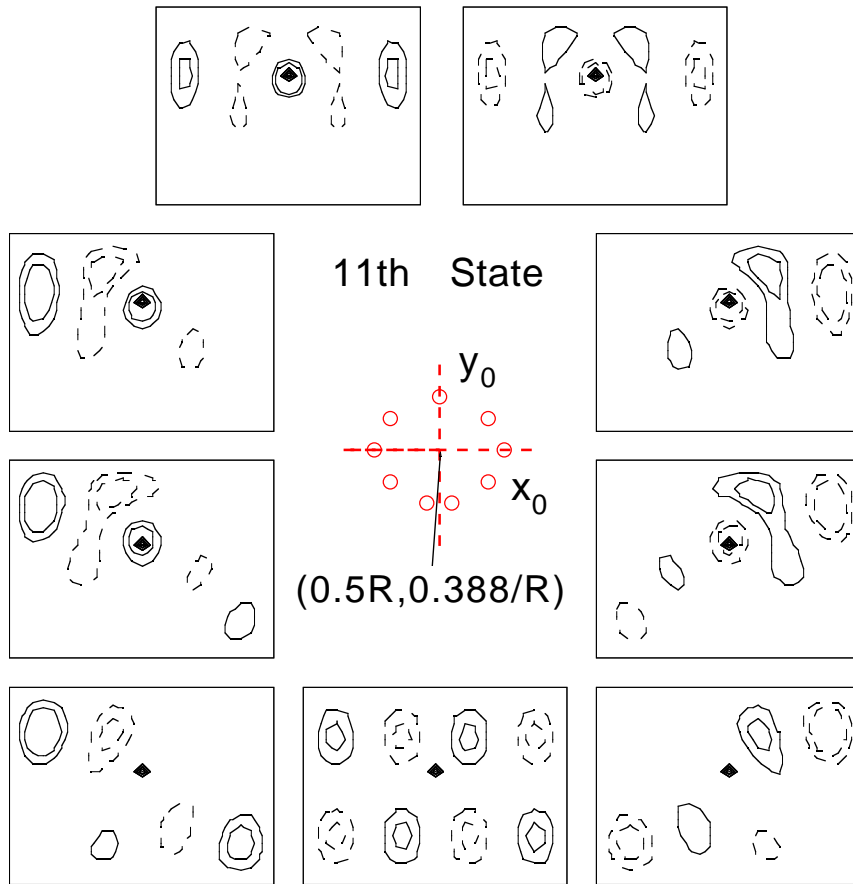


Fig. 4b